

# Dalton Transactions

Accepted Manuscript



This is an *Accepted Manuscript*, which has been through the Royal Society of Chemistry peer review process and has been accepted for publication.

*Accepted Manuscripts* are published online shortly after acceptance, before technical editing, formatting and proof reading. Using this free service, authors can make their results available to the community, in citable form, before we publish the edited article. We will replace this *Accepted Manuscript* with the edited and formatted *Advance Article* as soon as it is available.

You can find more information about *Accepted Manuscripts* in the [Information for Authors](#).

Please note that technical editing may introduce minor changes to the text and/or graphics, which may alter content. The journal's standard [Terms & Conditions](#) and the [Ethical guidelines](#) still apply. In no event shall the Royal Society of Chemistry be held responsible for any errors or omissions in this *Accepted Manuscript* or any consequences arising from the use of any information it contains.

## Synthesis, crystal structure and magnetic properties of a new copper oxo-antimony sulphate $\text{CuSb}_6\text{O}_8(\text{SO}_4)_2$

Iwan Zimmermann<sup>a</sup>, Reinhard K. Kremer<sup>b</sup> Shichao Hu<sup>a</sup>, and Mats Johansson<sup>a\*</sup>

a) Department of Materials and Environmental Chemistry, Stockholm University, SE-106 91 Stockholm, Sweden

b) Max Planck Institute for Solid State Research, Heisenbergstrasse 1, D-70569 Stuttgart, Germany

\* Corresponding author, Email: [mats.johansson@mmk.su.se](mailto:mats.johansson@mmk.su.se), tel: +46-8-162169, fax: +46-8-152187

### Abstract

The new copper oxo-antimony sulphate  $\text{CuSb}_6\text{O}_8(\text{SO}_4)_2$  crystallizes in the triclinic space group  $P-1$  with the unit cell parameters  $a = 5.5342(4)$  Å,  $b = 7.6706(6)$  Å,  $c = 9.2374(7)$  Å,  $\alpha = 96.505(5)^\circ$ ,  $\beta = 93.818(4)^\circ$ ,  $\gamma = 109.733(4)^\circ$  and  $Z = 1$ . The crystal structure is made up by layers stacking along  $[001]$ . The layers are charge neutral and connect to each other by only weak interactions. The copper atoms adopt a square planar  $[\text{CuO}_4]$  coordination and such units are well separated from each other by corner and edge sharing to  $[\text{SbO}_4]$  building blocks. The latter polymerize to form sheets with the formula  $[\text{Sb}_3\text{O}_8]_\infty$ . Sulphate groups connect to the antimony oxide sheets by corner sharing and are located at the interface of the layers. Above  $\sim 10$  K the magnetic susceptibility follows very well a Curie-Weiss law whereas below 10 K increasing deviations indicate onset of antiferromagnetic correlations. Fitting the data in the range 10 – 50 K yield a Curie-Weiss temperature  $\theta$  of  $-2.25(5)$  K. A sharp anomaly centered at  $T_C = 0.67$  K in the heat capacity data indicate long-range magnetic ordering. Short range antiferromagnetic correlations well above  $T_C$  are seen in the magnetic contribution to the heat capacity and the magnetic susceptibility. These can be well described by the magnetism of a spin  $S = 1/2$  Heisenberg chain with nearest neighbor antiferromagnetic spin exchange interaction of  $J_{\text{intra}} = \sim 2.8$  K.

## Introduction

Utilizing p-block elements having stereochemically active lone pair electrons as constituents **has proven to be a successful** synthesis concept for synthesizing new compounds with low dimensional arrangements. Because the lone pairs as *e.g.* realized in  $\text{Se}^{4+}$ ,  $\text{Te}^{4+}$ , and  $\text{Sb}^{3+}$  occupy non-bonded space in the crystal structure they adopt an asymmetric one-sided coordination.<sup>1</sup> Often the non-bonding electron pair acts as terminal ligand, which allows only weak van der Waals interactions. This concept was previously coined as “chemical scissors”, as the lone pair is able to slice and open up a crystal structure.<sup>2-3</sup>

Transition metal sulphates are usually soluble in water which makes hydrothermal **synthesis as the preferable synthesis method**. Sulphate groups form well defined tetrahedra which have shown to be suitable building blocks for materials exhibiting interesting physical and especially magnetic properties. Such a class of compounds are the jarosites with the general formula  $\text{AM}_3(\text{SO}_4)_2(\text{OH})_6$  (A = monovalent cation, M = trivalent metal ion), which are well known for forming unusual magnetic ground states due to the magnetic cations forming a frustrated kagomé lattice.<sup>4-6</sup> Ferromagnetic systems have also been observed.<sup>7</sup> Only some few compounds containing antimony in combination with sulphate groups have been reported previously. They show layered arrangements as in  $\text{K}_2\text{SO}_4(\text{SbF}_3)_2$ ,<sup>8</sup> chains as in  $\text{Sb}_2\text{O}_3 \cdot 3\text{SO}_3$ ,<sup>9</sup> or clusters as in  $\text{Sb}_2\text{O}_3 \cdot 2\text{SO}_3$  and the antimony disulphate  $\text{Sb}_2(\text{S}_2\text{O}_7)_3$ .<sup>10</sup> Here we report the synthesis, structural and magnetic properties of the new compound  $\text{CuSb}_6\text{O}_8(\text{SO}_4)_2$ . To the best of our knowledge  $\text{CuSb}_6\text{O}_8(\text{SO}_4)_2$  is the first oxo-antimony(III) sulphate compound containing a transition metal cation.

## Experimental Section

Single crystals of  $\text{CuSb}_6\text{O}_8(\text{SO}_4)_2$  were obtained by hydrothermal synthesis from a non-stoichiometric mixture of 0.9 g (3.1 mmol)  $\text{Sb}_2\text{O}_3$  (Sigma-Aldrich) and 0.45 g (2.8 mmol)  $\text{CuSO}_4$  (Sigma-Aldrich). The starting materials were put together with 10 ml deionized water in a 23 ml Teflon lined steel autoclave and allowed to react for 3 days at 200 °C. The autoclave was subsequently furnace cooled to room temperature. After filtration dark green crystals **in a yield of ~50%** were separated manually from unreacted  $\text{Sb}_2\text{O}_3$  for further analysis. Single crystal X-ray diffraction experiments were carried out on a Bruker D8 diffractometer equipped with a graphite monochromator. Data were collected at 293 K using  $\text{MoK}\alpha$  radiation,  $\lambda = 0.71073 \text{ \AA}$ . Absorption correction and data reduction were done with the software APEX 2 that was also employed for the multi-scan absorption correction.<sup>11</sup> The structure solution was carried out with the Superflip software implemented in the Jana2006

program package<sup>12</sup> and the refinement with SHELXL-97.<sup>13</sup> All atom positions were refined allowing anisotropic thermal displacement. The crystallographic data are reported in Table 1. The structural drawings are made with the program DIAMOND.<sup>14</sup>

Magnetic susceptibilities of a powder sample (~20 mg) were measured as a function of temperature with a MPMS SQUID magnetometer (Quantum Design, 6325 Lusk Boulevard, San Diego) with a home-built <sup>3</sup>He insert [Ref.: R. K. Kremer, *et al.*, to be published] in the temperature range 0.6 – 250 K. Heat capacities were determined on powder immersed in Apiezon N vacuum grease using the relaxation method implemented in a PPMS system (Quantum Design, 6325 Lusk Boulevard, San Diego) in the temperature range 0.4 – 100 K.

## Results and Discussion

### Crystal structure

The new transition metal oxo-antimony sulphate  $\text{CuSb}_6\text{O}_8(\text{SO}_4)_2$  crystallizes in the space group *P*-1. The crystal structure can be regarded as layered having the sulphate groups protruding from the layers. The layers are parallel to (110), see Figure 1. The copper ion adopts a  $[\text{CuO}_4]$  square planar coordination with Cu – O bond distances in the range 1.957(7) – 1.989(7) Å. The sulphate groups form regular tetrahedra with S – O bond lengths from 1.442(9) Å to 1.496(9) Å. There are three crystallographically independent antimony sites. They have an asymmetric one-sided coordination towards four oxygens due to the stereochemically active lone pair. All three antimony atoms form  $[\text{SbO}_{3+1}]$  units with three short Sb – O bonding distances ranging from 1.978(7) Å - 2.124(7) Å and one longer Sb – O bond 2.286(7) Å - 2.418(8) Å, see Figure 2 and Table 2. The antimony oxide building blocks polymerize to build layers in which the  $[\text{CuO}_4]$  square planes are embedded well separated from each other. Each sulphate group bond via two oxygens to antimonite groups in the same layer and has weak interactions via the other two oxygen atoms to antimonite groups in the next layer. Those longer interactions are just outside the primary coordination sphere (2.8 – 3.0 Å). Those terminal oxygen atoms (O7 and O8) have relatively large thermal ellipsoids. In the previously described framework compound  $\text{SbO}_4(\text{OH})_2\text{SO}_4$  two long Sb-O bonds (antimony – to sulphate) having bond distances of ~2.72 and ~2.89 Å are observed.<sup>15</sup> Similar arrangement is found also in  $\text{Sb}_6\text{O}_7(\text{SO}_4)_2$  where the oxygens protrude into small channels and have relatively high temperature factors.<sup>16</sup> A third example is the compound  $\text{Sb}_2(\text{S}_2\text{O}_7)_3$  where one oxygen atom in the sulphate group is weakly connected to Sb.<sup>17</sup>

### Magnetic and thermal properties

The molar magnetic susceptibility of  $\text{CuSb}_6\text{O}_8(\text{SO}_4)_2$  shown in Figure 3 was corrected for the temperature independent diamagnetic part according to  $\chi_{\text{mol}}^*(T) = \chi_{\text{mol}}(T) - \chi_{\text{dia}}$ , where the diamagnetic part per formula unit  $\text{CuSb}_6\text{O}_8(\text{SO}_4)_2$  was estimated from the increments listed in Selwood's table<sup>18</sup> to  $\chi_{\text{dia}} = -289 \times 10^{-6} \text{ cm}^3/\text{mol}$ .

The inset displays the inverse magnetic susceptibility which indicates Curie-Weiss behaviour above  $\sim 5$  K according to

$$\chi_{\text{mol}}^*(T) = \frac{C}{T - \Theta}, \quad (\text{Eq. 1})$$

where  $C$  is the Curie constant given by

$$C = \frac{N_A g^2 \mu_B^2 S(S+1)}{3k_B}, \quad (\text{Eq. 2})$$

and  $N_A$  is Avogadro's constant,  $g$  is the  $g$ -factor and  $\mu_B$  is the Bohr magneton.  $S$  is the spin of a  $\text{Cu}^{2+}$  ion associated to the electronic configuration ( $3d^9$ ),  $S = 1/2$ ,  $k_B$  is the Boltzmann constant and  $\Theta$  Curie-Weiss temperature. Fitting the experimental data to Eq. (1) indicates a  $g$ -factor of 2.14(1) implying an effective magnetic moment per Cu atom of  $1.85 \mu_B$ , in good agreement with typical powder-averaged values for  $\text{Cu}^{2+}$  cations in an octahedral oxygen environment.<sup>19</sup> The Curie-Weiss temperature,  $\Theta$ , amounts to  $-2.25(5)$  K indicating predominant antiferromagnetic spin exchange between the Cu moments.

The full temperature dependence of the magnetic susceptibility of  $\text{CuSb}_6\text{O}_8(\text{SO}_4)_2$  and especially the broad maximum centred at  $\sim 1.8$  K can be successfully modelled by the magnetic susceptibility of the  $S = 1/2$  Heisenberg chain with antiferromagnetic nearest-neighbour spin exchange interaction described by

$$H = J_{\text{intra}} \sum_i \vec{S}_i \vec{S}_{i+1}, \quad (\text{Eq. 3})$$

where  $J_{\text{intra}}$  is the intrachain antiferromagnetic spin exchange interaction between neighbouring spins and  $\vec{S}_i$ , and  $\vec{S}_{i+1}$  are the associated spin operators. The susceptibility of the  $S = 1/2$  Heisenberg chain with antiferromagnetic nearest-neighbour spin exchange interaction has been calculated by Quantum Monte Carlo simulations and transfer-matrix density-matrix renormalization group calculations to high precision. Johnston *et al.* encoded these data into a Padé approximant the coefficients of which are tabulated.<sup>20</sup> In order to allow interchain spin exchange interaction which generally induce long range magnetic ordering at low temperatures we utilized the following molecular field theory description for the susceptibility

$$\chi_{\text{mol}}^{\text{MF}}(T) = \frac{\chi_{\text{mol}}^{\text{chain}}(T)}{1 + (z' J_{\text{inter}} / N_{\text{A}} g^2 \mu_{\text{B}}^2) \chi_{\text{mol}}^{\text{chain}}(T)}, \quad (\text{Eq. 4})$$

where  $\chi_{\text{mol}}^{\text{chain}}(T)$  represents the molar magnetic susceptibility of the antiferromagnetic Heisenberg chain and  $J_{\text{inter}}$  the interchain spin exchange interaction to  $z'$  neighbors.<sup>19-20</sup> Figure 3 (main frame) highlights the fit of Eq. 4 to the experimental data with an antiferromagnetic intrachain spin exchange interaction of 2.12(1) K, a g factor of 2.12(1). The value of 0.33(1) K for the product  $z' J_{\text{inter}}$  indicates an antiferromagnetic interchain exchange which is about an order of magnitude smaller than the intrachain spin exchange interaction. A closer inspection of the susceptibilities below 1 K (Figure 3, lower inset) reveals a kink at 0.69(2) K possibly due to the onset of long range magnetic order.

Long-range magnetic ordering is especially evidenced by a sharp anomaly centered at  $T_{\text{C}} = 0.67$  K in the specific heat data displayed in Figure 4 in good agreement with the value expected from the susceptibility data. Above the sharp anomaly a shoulder appears and magnetic contributions to the heat capacity can be identified to temperatures of approximately 10 K. The magnetic entropy contained in this sharp anomaly and the broad shoulder amounts to  $\sim 5.4$  J/mol K or approximately 94% of the magnetic entropy expected for the ordering of a  $S = 1/2$  spin system ( $R \ln 2$ , where R is the molar gas constant). The major fraction of the entropy is already removed by short range magnetic ordering spread out over an extended temperature range above  $T_{\text{C}}$ . Figure 5 displays the heat capacity of  $\text{CuSb}_6\text{O}_8(\text{SO}_4)_2$  together with a fit assuming a superposition of a lattice contribution to the heat,  $C_{\text{lat}}(T)$ , and a magnetic contribution,  $C_{\text{mag}}(T)$  according to

$$C_P(T) = C_{\text{mag}}(T) + C_{\text{lat}}(T). \quad (\text{Eq. 5})$$

For  $C_{\text{mag}}(T)$  we take the heat capacity of a spin  $S = 1/2$  Heisenberg chain with uniform nearest-neighbor spin exchange interaction encoded into a Padé approximation by Johnston *et al.*<sup>18</sup> The lattice heat capacity  $C_{\text{lat}}(T)$  is approximated by a Debye-power law according to

$$C_{\text{lat}}(T) = \beta T^3 + \delta T^5 + \gamma T^7. \quad (\text{Eq. 6})$$

The fits reproduce very well the experimental data with an antiferromagnetic nearest-neighbor intrachain spin exchange interaction of  $J_{\text{intra}} = 2.85(5)$  K. The coefficient  $\beta$  in Eq. (6) is related to the Debye temperature  $\theta_{\text{Deb}}(T \rightarrow 0)$  according to Eq. (7), where  $n$  is the number of atoms in the formula unit (here  $n = 25$ ). With  $\beta = 0.00367(3)$  J/molK<sup>4</sup> one arrives at a Debye temperature of  $\theta_{\text{Deb}}(T \rightarrow 0) = 236(1)$  K.

$$\beta = n \frac{12}{5} \pi^4 R (1/\theta_{\text{Deb}})^3, \quad \text{Eq. (7)}$$

The complexity of the crystal structure of  $\text{CuSb}_6\text{O}_8(\text{SO}_4)_2$  leaves it very difficult to assign clear preferential spin exchange pathways. Our experimental results and the good agreement with the theoretical data expected for the  $S = 1/2$  nearest-neighbor antiferromagnetically coupled Heisenberg chain, however, clearly indicate substantially anisotropic spin exchange which support one-dimensional magnetic behaviour. Interchain spin exchange is found to be an order of magnitude smaller and leads to long-range antiferromagnetic ordering below 0.69 K.

## Conclusion

The new copper oxo-antimony sulphate  $\text{CuSb}_6\text{O}_8(\text{SO}_4)_2$  has been synthesized and its structural and magnetic properties have been characterized. It crystallizes in the triclinic space group  $P-1$  and the crystal structure is made up by layers stacking along [001]. The layers are charge neutral and connect to each other by only weak interactions. The copper atoms adopt a square planar  $[\text{CuO}_4]$  coordination and such units are well separated from each other by corner and edge sharing to  $[\text{SbO}_4]$  building blocks that polymerize to form sheets with the formula  $[\text{Sb}_3\text{O}_8]_{\infty}$ . Sulphate groups connect to the antimony oxide sheets by corner sharing and are located at the interface of the layers. Magnetic susceptibility and heat capacity data

agree very well and indicate an antiferromagnetic intrachain spin exchange interaction of  $\sim 2.8$  K. Clear signatures of long-range antiferromagnetic ordering below  $\sim 0.7$  K are observed in the magnetic susceptibility data as well as in the heat capacity data. The analysis of the magnetic susceptibility data allows estimating the interchain spin exchange interaction which is found to be one order of magnitude smaller than the interchain spin exchange interaction.

### **Acknowledgement**

This work has in part been carried out through financial support from the Swedish Research Council. We thank E. Brücher, S. Höhn and G. Siegle for expert experimental assistance.

### **Supporting Information**

Further details on the crystal structural investigations can be obtained from the Fachinformationszentrum Karlsruhe, Abt. PROKA, 76344 Eggenstein-Leopoldshafen, Germany (fax +49-7247-808-666; E-mail: [crysdata@fiz-karlsruhe.de](mailto:crysdata@fiz-karlsruhe.de)) by quoting the depository number CSD-428356.



## References

1. J. Galy, G. Meunier, S. Andersson, A. Åsröm, *J. Solid State Chem.* 1975, **13**, 142-159.
2. R. Becker, M. Johnsson, R. Kremer, P. Lemmens, *Solid State Sciences*, 2003, **5**, 1411-1416.
3. V. Jo, M.K. Kim, D.W. Lee, I.-w. Shim, K.M. Ok, *Inorg. Chem.* 2010, **49**, 2990-2995.
4. A.V. Powell, P. Leyva-Bailen, P. Vaqueiro and R.D. Sanchez, *Chem. Mater.* 2009, **21**, 4102-4104.
5. W.G. Bisson and A.S. Wills, *J. Phys.: Condens. Matter*, 2008, **20**, 452204.
6. A.P.C. Ramirez, C. Broholm, S.H. Lee, M.F. Collins, L. Heller, C. Kloc and E. Bucher, *J. Appl. Phys.*, 1993, **73**, 5658.
7. D. Grohol, D. Papoutsakis and D.G. Nocera, *Angew. Chem. Int. Ed.*, 2001, **40**, 1519-1521.
8. M. Bourgault, B. Ducourant, B. Bonnet and R. Fourcade, *J. Solid State Chem.*, 1981, **36**, 183-189.
9. P.R. Mercier, J. Douglade and J. Bernard, *Acta Cryst. B*, 1976, **B32**, 2787-2791.
10. a) P.R. Mercier, J. Douglade and F. Theobald, *Acta Cryst. B*, 1975, **B31**, 2081-2085; b) P.J. Douglade and R. Mercier, *Acta Cryst. B*, 1979, **B35**, 1062-1067.
11. Bruker, 2007, APEX 2. Bruker AXS Inc., Madison, Wisconsin, USA.
12. V. Petricek, M. Dusek and L. Palatinus, Institute of Physics, Praha, Czech Republic, 2006.
13. G.M. Sheldrick, *Acta Crystallogr.* 2008, **A64**, 112-122.
14. G. Bergerhoff, 1996, DIAMOND, Bonn, Germany.
15. S. Menchetti and C. Sabelli, *American Mineralogist*, 1980, **65**, 931-935.
16. J.-O. Bovin, *Acta Cryst.* 1976, **B32**, 1771-1777.
17. P.J. Douglade and R. Mercier, *Acta Materialia*, 1979, **B35**, 1062-1067.
18. P.W. Selwood, *Magnetochemistry*, 2<sup>nd</sup> edition, Interscience, New York 1956.
19. R.L. Carlin, *Magnetochemistry*, Springer Verlag, Berlin Heidelberg New York, 1986.
20. D.C. Johnston, R.K. Kremer, M. Troyer, X. Wang, A. Klümper, L. Bud'ko, A.F. Panchula, and P.C. Canfield, *Phys. Rev. B*, 2000, **61**, 9558-9606.

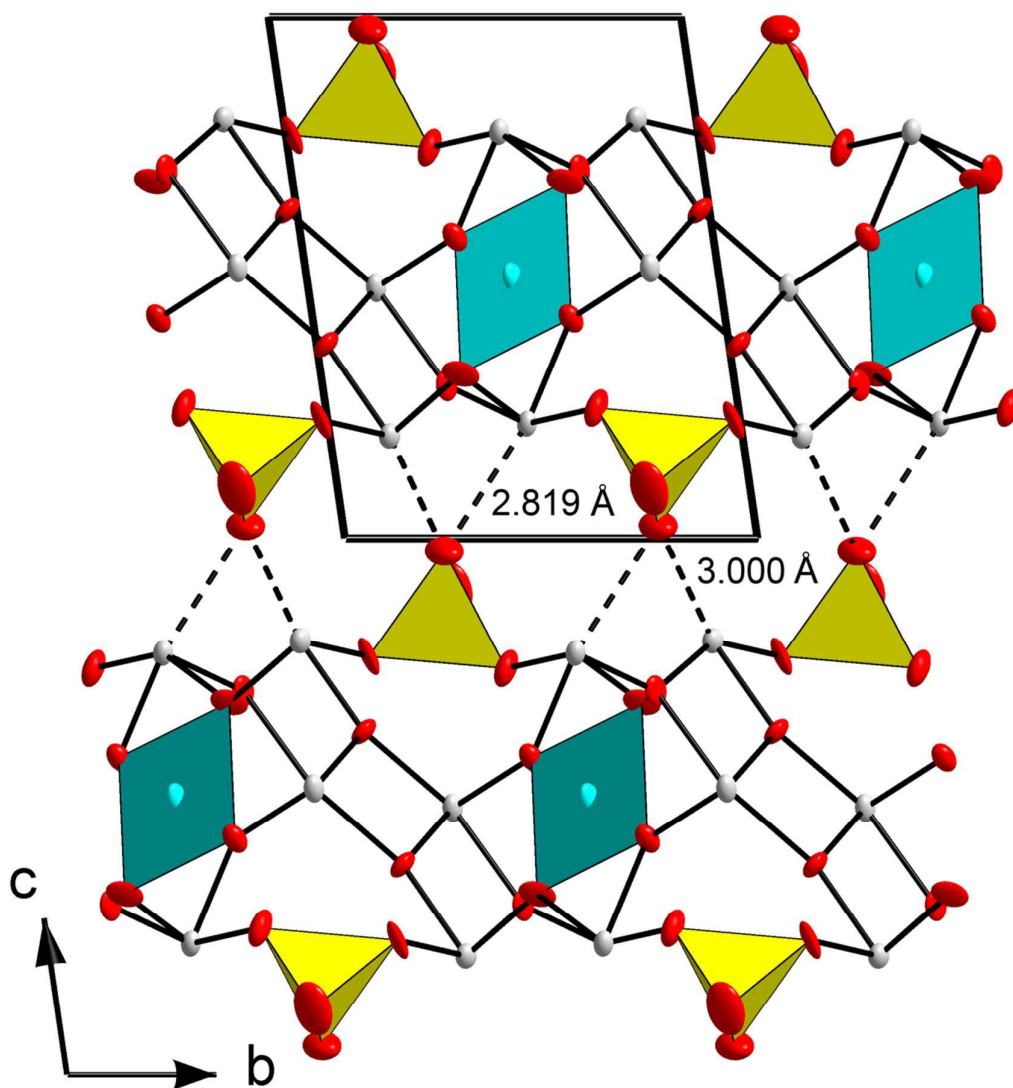
**Table 1** Crystallographic data for  $\text{CuSb}_6\text{O}_8(\text{SO}_4)_2$ .

Crystal system	triclinic
Space group	$P\bar{1}$
Temperature / K	293(3)
Lattice constants / Å and °	a = 5.5342(4) b = 7.6706(6) c = 9.2374(7) $\alpha = 96.505(5)$ $\beta = 93.818(4)$ $\gamma = 109.733(4)$
Volume / Å <sup>3</sup>	364.42(5)
Z	1
Dcalculated / g·cm <sup>-3</sup>	5.077
Radiation	Mo-K $\alpha$ ( $\lambda = 0.71073$ Å)
Crystal dimensions / mm	0.019 × 0.027 × 0.066
$\Theta$ range / °	2.85 – 26.37
Min. / max. h k l	$-6 \leq h \leq 6$ $-9 \leq k \leq 9$ $-11 \leq l \leq 11$
Reflections, measured	7313
Reflections, independent	1483
Absorption coefficient / mm <sup>-1</sup>	12.76
Absorption correction	Multi-scan
Refined parameters	115
R1 [ $I > 2\sigma(I)$ ]	0.0339
wR2 (all data)	0.0858
Max. / min. residual	2.129 and -1.339
Density / e <sup>-</sup> /Å <sup>3</sup>	

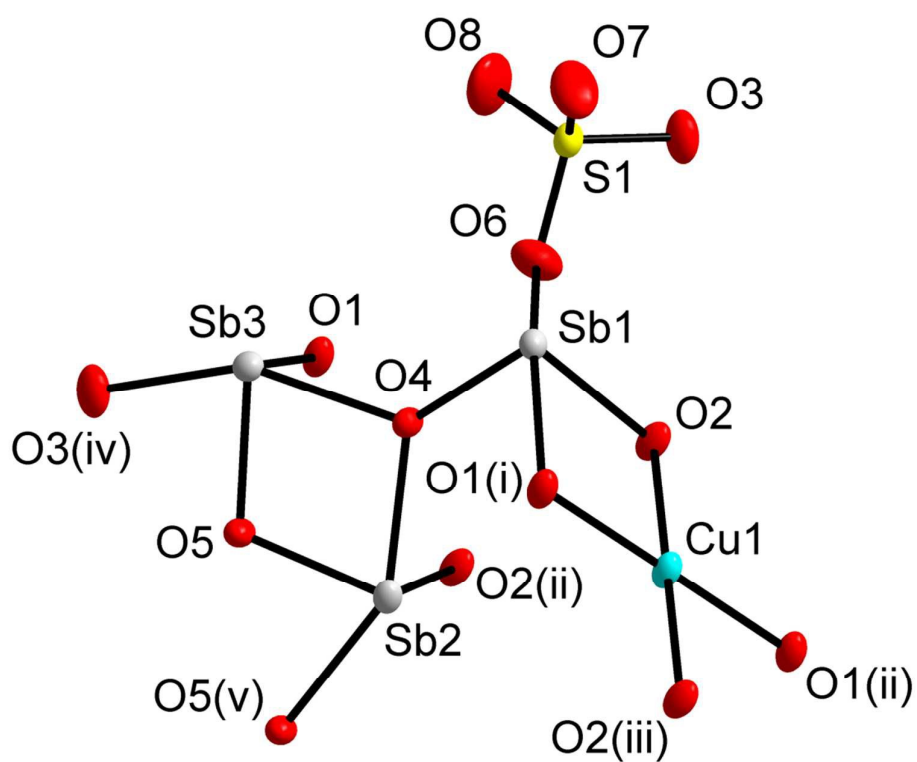
**Table 2** Selected bond lengths / Å for CuSb<sub>6</sub>O<sub>8</sub>(SO<sub>4</sub>)<sub>2</sub>.

Sb1 – O1i	2.102(7)	Sb3 – O4	2.124(7)
Sb1 – O2	2.037(7)	Sb3 – O5	1.997(7)
Sb1 – O4	2.002(7)	Cu1 – O1i	1.957(7)
Sb1 – O6	2.418(8)	Cu1 – O1ii	1.957(7)
Sb2 – O2ii	2.008(7)	Cu1 – O2	1.989(7)
Sb2 – O4	2.122(7)	Cu1 – O2v	1.989(7)
Sb2 – O5	2.008(7)	S1 – O3	1.490(8)
Sb2 – O5iii	2.286(7)	S1 – O6	1.496(9)
Sb3 – O1	1.978(7)	S1 – O7	1.458(9)
Sb3 – O3iv	2.347(8)	S1 – O8	1.442(9)

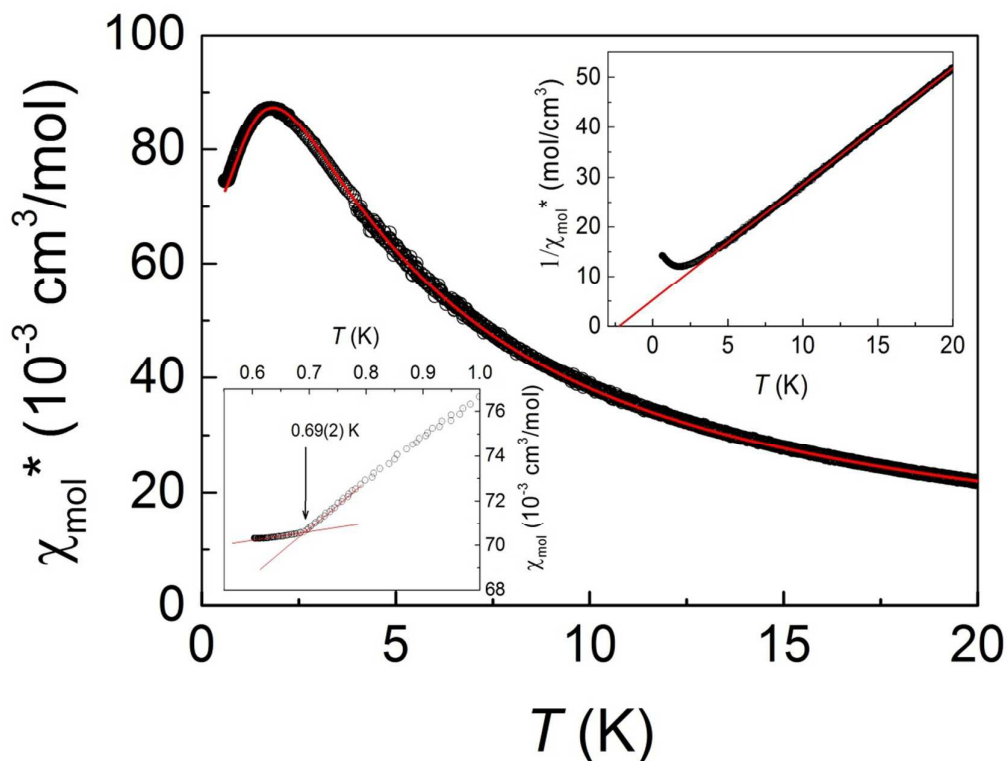
Note: Symmetry codes: (i)  $x-1, y, z$ ; (ii)  $-x+1, -y+1, -z+1$ ; (iii)  $-x+1, -y, -z+1$ ; (iv)  $x, y-1, z$ ; (v)  $-x, -y+1, -z+1$ .



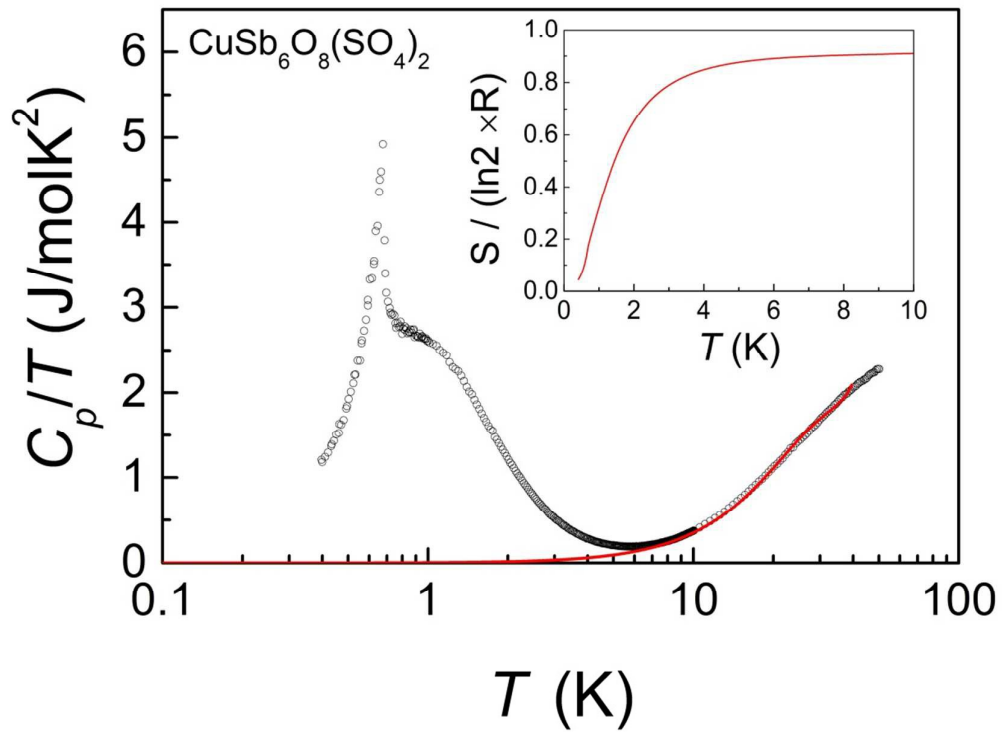
**Figure 1** Crystal structure of  $\text{CuSb}_6\text{O}_8(\text{SO}_4)_2$  projected along  $[100]$ . Long  $\text{Sb}\cdots\text{O}$  interactions responsible for layer cohesion are indicated with dashed lines. Color codes: grey: Sb; cyan: Cu; yellow: S; red: oxygen.



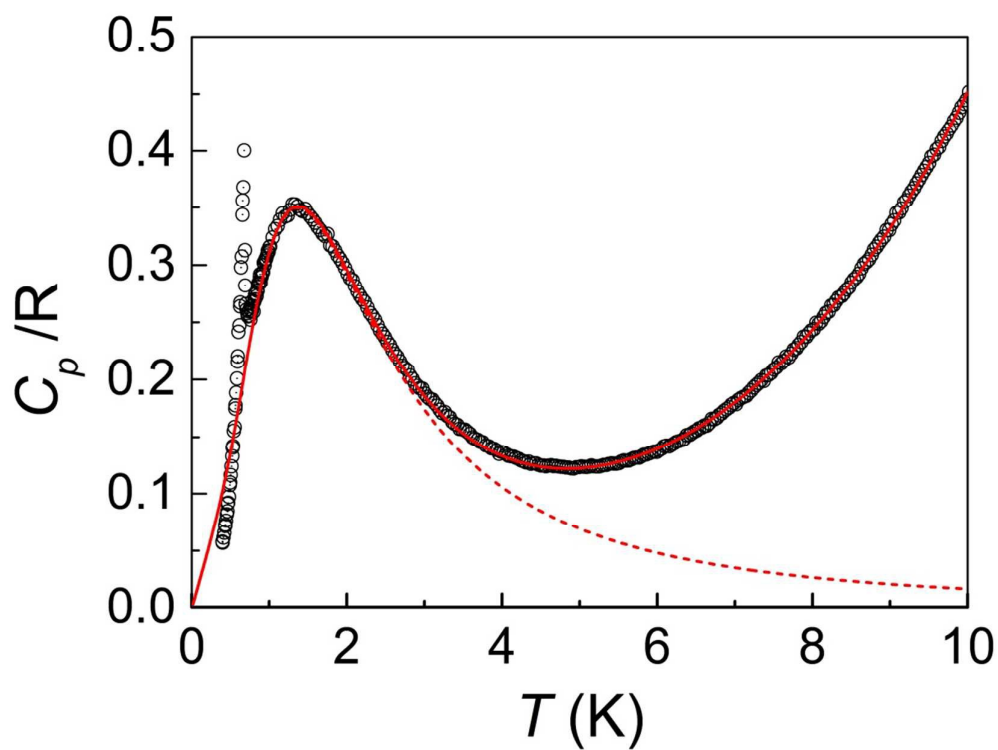
**Figure 2** Asymmetric unit and selected symmetry equivalents of  $\text{CuSb}_6\text{O}_8(\text{SO}_4)_2$ . Symmetry codes: (i)  $x-1, y, z$ ; (ii)  $-x+1, -y+1, -z+1$ ; (iii)  $-x, -y+1, -z+1$ ; (iv)  $x, y-1, z$ ; (v)  $-x+1, -y, -z+1$ ; (vi)  $-x+1, -y+1, -z$ .



**Figure 3** (Main frame) Molar magnetic susceptibility of  $\text{CuSb}_6\text{O}_8(\text{SO}_4)_2$  corrected for a diamagnetic contribution according to  $\chi_{\text{mol}}^*(T) = \chi_{\text{mol}}(T) - \chi_{\text{dia}}$ . The red solid line represents a fit of the experimental data to the susceptibility of the  $S=1/2$  Heisenberg chain with a nearest neighbor antiferromagnetic spin exchange of  $2.78(1)$  K and a  $g$  factor of  $2.12(1)$ . A mean field-type correction with an antiferromagnetic interchain coupling strength of  $z'J_{\text{inter}} = 0.33(1)$  K was applied (for more details see text). (Upper inset) Inverse molar susceptibility fitted to a Curie-Weiss law above 5 K. The negative intersection with the abscissa indicates predominant antiferromagnetic spin exchange interaction. (Lower inset) Low-temperature part of the molar magnetic susceptibility of  $\text{CuSb}_6\text{O}_8(\text{SO}_4)_2$  highlighting the kink at  $0.69(1)$  K due to the onset of long-range antiferromagnetic ordering.

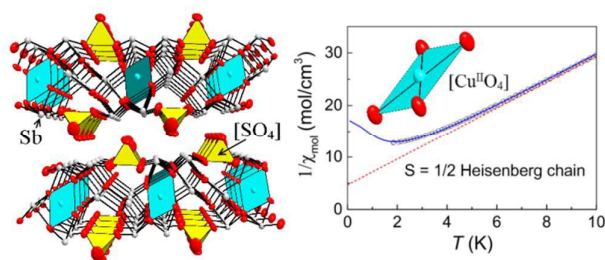


**Figure 4** Heat capacity of  $\text{CuSb}_6\text{O}_8(\text{SO}_4)_2$  showing onset of long-range order at 0.67 K. The red solid line shows the lattice contribution obtained by fitting the data above 10 K to a polynomial (see text) and extrapolating to  $T \rightarrow 0$  K. The inset displays the magnetic entropy obtained by integrating  $C_{\text{mag}}(T)/T$ .



**Figure 5** Heat capacity of  $\text{CuSb}_6\text{O}_8(\text{SO}_4)_2$ . The solid red line shows the results of a fit of the experimental data ( $T > 0.75$  K) to Eq. (4). The dashed red line shows the magnetic contribution of a  $S = 1/2$  Heisenberg chain with uniform intrachain nearest neighbour spin exchange of  $2.85(5)$  K. Below  $0.75$  K the fit was extrapolated to  $T \rightarrow 0$  K.



**For Table of Contents Only**

The new compound  $\text{CuSb}_6\text{O}_8(\text{SO}_4)_2$  was synthesised by hydrothermal methods at  $200^\circ\text{C}$ . The crystal structure is made up from charge neutral layers with long antimony oxygen distances present in between the layers. Heat capacity measurements show a phase transition at  $0.67$  K, which are due to antiferromagnetic interaction in between the  $\text{Cu}^{2+}$  atoms. The magnetic susceptibility could be fitted to a spin  $S = 1/2$  Heisenberg chain model with  $J \sim 32.8\text{K}$ .